*Inorg. Chem.* **2003**, *42*, 5252–5258

# Influence of the Ligand on the Coupling between the Metal-Based Electrons in Face-Shared $[M_2X_9]^{3-}$ (M = Mo, W; X = F, Cl, Br, I) Systems

**Germán Cavigliasso† and Robert Stranger***

*Department of Chemistry, Faculty of Science, Australian National University, Canberra ACT 0200, Australia*

Received December 20, 2002

Orbital overlap and spin polarization effects in Mo and W $[M_2X_9]^{3-}$ halide and in $[M_2X'_3X''_6]^{3-}$ mixed-halide systems have been investigated by means of density-functional calculations performed on the $S = 0$, $S = 3$, and reference states of these species. For the regular $[M_2X_9]^{3-}$ systems, a strong linear correlation between the two factors has been obtained, and decreasing trends in both the overlap energy and the spin polarization energy upon descending the halide group have been observed. These trends can be related to the changes in the size and covalency of the ligands and in the nature of the metal–bridge interaction. For the mixed-ligand $[M_2X'_3X''_6]^{3-}$ systems, important deviations (from the behavior of the regular systems), which are apparently the result of particular structural and energetic characteristics, have been observed.

## 1. Introduction

The bonding in face-shared dinuclear metal systems (or $[M_2X_9]^{z-}$ "dimers") is distinctively characterized by the range of interactions possible between the two metal centers.[1,2] This is appropriately exemplified by the transition elements of group 6, for which the strength of the metal−metal interactions varies from strong multiple bonding observed in $[W_2Cl_9]^{3-}$ to weak antiferromagnetic coupling in $[Cr_2Cl_9]^{3-}$.

Two factors can be considered central to determining the strength of the interaction between the metal atoms.[2] These are the overlap between the orbitals on opposite metal centers, and the exchange or (spin polarization) energy associated with the presence of unpaired electron density. Significant overlap of the metal orbitals favors electron delocalization, whereas the spin polarization energy favors electron localization.

In a previous publication,[2] we have explored the electronic and structural properties of a variety of $[M_2Cl_9]^{z-}$ (M= Cr, Mo, W, Mn, Tc, Re) dimers with the $d^3d^3$ metal configuration, and we have also considered mixed-metal systems with $[M'M''Cl_9]^{z-}$ formulas, where M′ and M″ represent metals in the same group. The focus of this earlier work has been the identification of the properties of the individual metal ions that determine whether the electrons are localized or delocalized in the dimer, and how these factors vary across the periodic table.

We have found that the greater radial expansion of the d orbitals in the heavier metals of a given group reduces the spin polarization energy and increases the overlap between orbitals on adjacent centers, and both factors contribute to the increased tendency of the metal-based electrons to delocalize as the group is descended. Across a period, the metals of group 7 exhibit a greater tendency toward localization than the metals of group 6, due to decreased orbital overlap (associated with the more contracted nature of the d orbitals) prevailing over decreased spin polarization (resulting from the greater covalency of the M−Cl bonds).

The majority of our work on $[M_2X_9]^{z-}$ systems has concentrated on chloride dimers, but recently we have also investigated the ligand dependence of metal−metal bonding in $d^3d^3$ dimers through a detailed analysis of the potential energy surfaces of systems containing F, Cl, Br, and I ligands.[3] In this Article, we extend the study of the ligand dependence of metal−metal bonding by exploring orbital overlap and spin polarization effects in Mo and W $[M_2X_9]^{3-}$ (X = F, Cl, Br, I) systems, and also in $[M_2X'_3X''_6]^{3-}$ mixed-ligand species.

* Author to whom correspondence should be addressed. E-mail: Rob.Stranger@anu.edu.au.
† E-mail: German.Cavigliasso@anu.edu.au.

(1) McGrady, J. E.; Stranger, R.; Lovell, T. *J. Phys. Chem. A* **1997**, *101*, 6265.
(2) McGrady, J. E.; Lovell, T.; Stranger, R. *Inorg. Chem.* **1997**, *36*, 3242.
(3) Stranger, R.; Turner, A.; Delfs, C. D. *Inorg. Chem.* **2001**, *40*, 4093.



10.1021/ic026291p CCC: $25.00 © 2003 American Chemical Society
Published on Web 07/26/2003

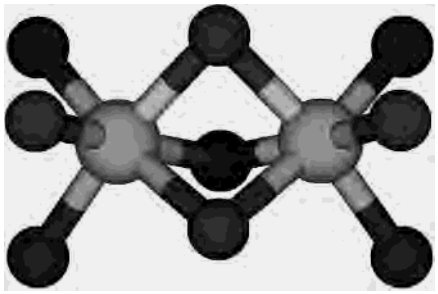

**Figure 1.** Molecular structure of face-shared $[M_2X_9]^{z-}$ systems.

## 2. Computational Approach

In a number of recent publications,[1−9] we have shown that a satisfactory description of the entire range of metal−metal interactions in face-shared $[M_2X_9]^{z-}$ dimers can be achieved by means of an approach based on analyzing the broken-symmetry potential energy curves in terms of the curves for the corresponding associated states.

For $d^3d^3$ face-shared $[M_2X_9]^{3-}$ dimers (Figure 1), symmetry breaking results in the lowering of the molecular symmetry from $D_{3h}$ to $C_{3v}$ as a consequence of removing all symmetry elements connecting the metal centers. The correlation between $C_{3v}$ and $D_{3h}$ molecular orbital descriptions is summarized by the scheme in part a of Figure 2.

The electronic configurations of the broken-symmetry state and of the corresponding $S = 0$, $S = 2$, and $S = 3$ associated states are given in part b of Figure 2. The antiferromagnetic configuration corresponding to the broken-symmetry state, represented by $[(a_1\uparrow)^1(a_1\downarrow)^1(e\uparrow)^2(e\downarrow)^2(a_1\uparrow)^0(a_1\downarrow)^0(e\uparrow)^0(e\downarrow)^0]$ in $C_{3v}$ symmetry, spans all possible degrees of delocalization of the $\sigma$ and $\delta_\pi$ electrons. The associated states correspond to different occupations of the metal−metal bonding and antibonding orbitals in $D_{3h}$ symmetry. The $S = 0$ state can be represented by the $[(a_1'\uparrow)^1(a_1'\downarrow)^1(e'\uparrow)^2(e'\downarrow)^2(e''\uparrow)^0(e''\downarrow)^0(a_2''\uparrow)^0(a_2''\downarrow)^0]$ configuration and is characterized by the strong coupling of the $\sigma$ and $\delta_\pi$ electrons (with a formal bond order of 3). Successive decoupling of these subsets of electrons leads to the $S = 2$ state, corresponding to paired $\sigma$ but decoupled $\delta_\pi$ electrons (with a formal bond order of 1) and described by the $[(a_1'\uparrow)^1(a_1'\downarrow)^1(e'\uparrow)^2(e'\downarrow)^0(e''\uparrow)^2(e''\downarrow)^0(a_2''\uparrow)^0(a_2''\downarrow)^0]$ configuration, and to the $S = 3$ state, represented by the $[(a_1'\uparrow)^1(a_1'\downarrow)^0(e'\uparrow)^2(e'\downarrow)^0(e''\uparrow)^2(e''\downarrow)^0(a_2''\uparrow)^1(a_2''\downarrow)^0]$ configuration in which all $\sigma$ and $\delta_\pi$ electrons are unpaired (or ferromagnetically coupled with a formal bond order of 0).

The calculation of the orbital overlap and spin polarization effects is connected with the $S = 0$ and $S = 3$ states represented in Figure 2, and also requires the definition of a suitable reference state.[2] The $S = 0$ state possesses a metal−metal triple bond but no spin polarization energy, whereas the $S = 3$ state has no metal−metal bond but has an excess of three electrons per metal center, and is thus stabilized solely by spin polarization effects. Therefore, the depths of the $S = 0$ and $S = 3$ curves can be equated, respectively, with the contributions due to orbital overlap and spin polarization.

In order to obtain the depths of the $S = 0$ and $S = 3$ curves, it is necessary to define a reference state in which the contributions from orbital overlap and spin polarization are negligible. This is schematically represented in Figure 3. The reference state corresponds to the $[(a_1'\uparrow)^{1/2}(a_1'\downarrow)^{1/2}(e'\uparrow)^1(e'\downarrow)^1$-

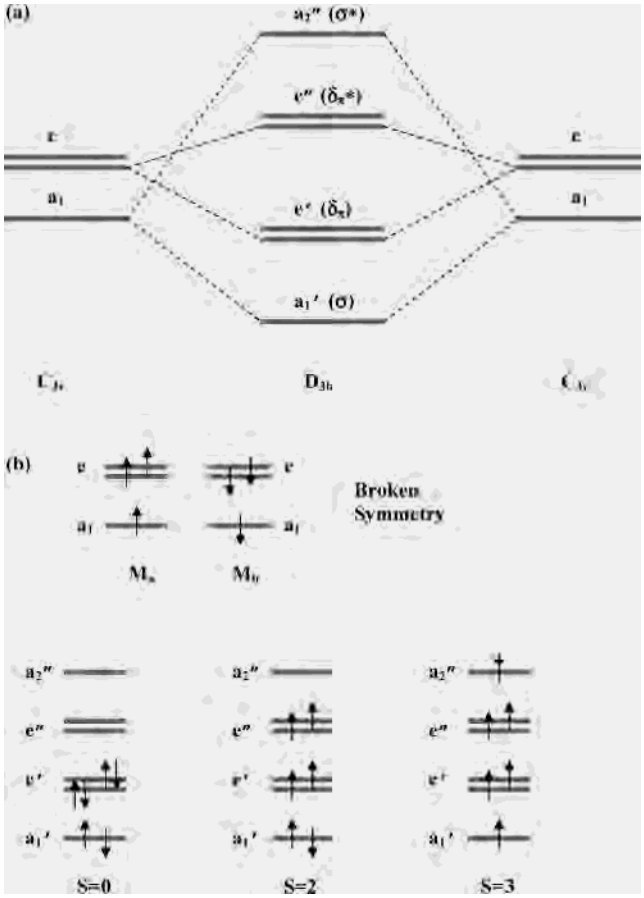


**Figure 2.** Schematic representations for (a) the correlation between metal-based molecular orbitals in $C_{3v}$ (broken symmetry) and $D_{3h}$ (full symmetry) descriptions, and (b) the electronic configuration of the broken-symmetry state and the $S = 0$, $S = 2$, and $S = 3$ associated states.

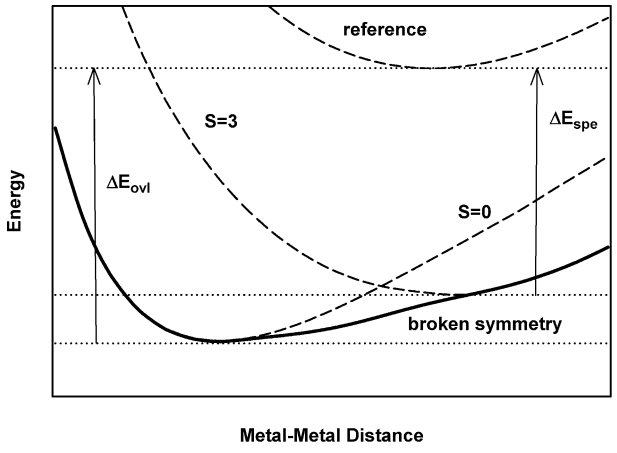


**Figure 3.** Schematic definition of the overlap ($\Delta E_{ovl}$) energy and spin polarization ($\Delta E_{spe}$) energy in relation to the $S = 0$, $S = 3$, and reference states of $d^3d^3$ $[M_2X_9]^{3-}$ systems.

(4) Lovell, T.; McGrady, J. E.; Stranger, R.; Macgregor, S. A. *Inorg. Chem.* **1996**, *35*, 3079.
(5) McGrady, J. E.; Stranger, R.; Lovell, T. *Inorg. Chem.* **1998**, *37*, 3802.
(6) Stranger, R.; McGrady, J. E.; Lovell, T. *Inorg. Chem.* **1998**, *37*, 6795.
(7) Lovell, T.; Stranger, R.; McGrady, J. E. *Inorg. Chem.* **2001**, *40*, 39.
(8) Petrie, S.; Stranger, R. *Polyhedron* **2002**, *21*, 1163.
(9) Stranger, R.; Petrie, S. *J. Chem. Soc., Dalton Trans.* **2002**, 3630.

$(e''\uparrow)^1(e''\downarrow)^1(a_2''\uparrow)^{1/2}(a_2''\downarrow)^{1/2}]$ configuration, and differs from the $S = 0$ state only in that it has no metal−metal bond, and from the $S = 3$ state only in that it has no spin polarization energy.

The separation between the reference and $S = 0$ states can be used to define the orbital overlap ($\Delta E_{ovl}$) contribution, whereas the separation between the reference and $S = 3$ states can be associated with the spin polarization ($\Delta E_{spe}$) contribution. The difference between these terms ($\Delta E_{spe} - \Delta E_{ovl}$) represents the energetic separation between the depths of the $S = 0$ and $S = 3$ curves, and can be considered a measure of the tendency of the metal-based electrons to localize.

## 3. Calculation Details

All density-functional calculations reported in this work were carried out with the ADF (2002.01) program.[10−12] Functionals based on the Volko−Wilk−Nusair[13] (VWN) form of the local density approximation[14] (LDA) were utilized for geometry optimizations, and no gradient corrections were included as previous work has shown that these normally result in poorer agreement with experimental structural data.[1] Basis sets of triple-$\zeta$ quality and one polarization function (TZP or type IV), incorporating frozen cores (Mo.3d, W.4f, F.1s, Cl.2p, Br.3p, I.4p), were employed.[10−12]

Additional calculations were performed on the W systems using ZORA scalar relativistic corrections.[10−12] The basis sets employed were of triple-$\zeta$ quality and two polarization functions (TZ2P or type V), with frozen cores equivalent to those described in the preceding paragraph.

Calculations on the reference, $S = 0$, and $S = 3$ states of $[M_2X_9]^{3-}$ species utilized the (full) $D_{3h}$ molecular symmetry. For comparison, calculations were also carried out on the broken-symmetry states of $[M_2X_9]^{3-}$ systems (using $C_{3v}$ molecular symmetry) and on the spin singlet and quartet states of the corresponding monomeric $[MX_6]^{3-}$ complexes (using $O_h$ molecular symmetry). These states of the $[MX_6]^{3-}$ complexes are chararacterized by the $[(t_{2g}\uparrow)^{3/2}(t_{2g}\downarrow)^{3/2}]$ and $[(t_{2g}\uparrow)^3(t_{2g}\downarrow)^0]$ configurations, respectively.

A fragment analysis was carried out to evaluate the effects of the metal−metal and metal−bridge interactions on the bonding energy of the $[M_2X_9]^{3-}$ systems. The approach described in a previous publication was utilized.[3] The fragment calculations were performed using the corresponding LDA geometry, but the gradient corrections proposed by Becke (1988)[15] and Perdew (1986)[16] were incorporated.

## 4. Results and Discussion

Optimized metal−metal bond distances and total bonding energy values for the reference, $S = 0$, and $S = 3$ states of the $[M_2X_9]^{3-}$ species are shown in Tables 1 and 2 for the Mo and W systems, respectively. The results of broken-symmetry calculations are also included, for comparison. The values of the structural parameters are similar to those reported in our previous publication.[3]

**Table 1.** Optimized Metal−Metal Bond Distance (M−M in Å) and Total Bonding Energy ($E_B$ in eV) for the Reference (RS), $S = 0$, $S = 3$, and Broken-Symmetry (BS) States of $[Mo_2X_9]^{3-}$ Species

| molecule | state | M−M | $E_B$ |
|---|---|---|---|
| $[Mo_2F_9]^{3-}$ | RS | 3.082 | −61.25 |
| | $S = 0$ | 2.215 | −64.85 |
| | $S = 3$ | 3.091 | −63.68 |
| | BS | 2.215 | −64.85 |
| $[Mo_2Cl_9]^{3-}$ | RS | 3.401 | −48.60 |
| | $S = 0$ | 2.395 | −51.41 |
| | $S = 3$ | 3.406 | −50.78 |
| | BS | 2.395 | −51.41 |
| $[Mo_2Br_9]^{3-}$ | RS | 3.574 | −44.63 |
| | $S = 0$ | 2.448 | −47.16 |
| | $S = 3$ | 3.551 | −46.73 |
| | BS | 2.663 | −47.15 |
| $[Mo_2I_9]^{3-}$ | RS | 3.741 | −40.09 |
| | $S = 0$ | 2.489 | −42.27 |
| | $S = 3$ | 3.747 | −42.07 |
| | BS | 3.054 | −42.31 |

**Table 2.** Optimized Metal−Metal Bond Distance (M−M in Å) and Total Bonding Energy ($E_B$ in eV) for the Reference (RS), $S = 0$, $S = 3$, and Broken-Symmetry (BS) States of $[W_2X_9]^{3-}$ Species[a]

| molecule | state | M−M | $E_B$ |
|---|---|---|---|
| $[W_2F_9]^{3-}$ | RS | 3.173 (3.212) | −62.37 (−60.98) |
| | $S = 0$ | 2.285 (2.245) | −66.30 (−65.58) |
| | $S = 3$ | 3.154 (3.182) | −64.62 (−63.18) |
| | BS | 2.285 (2.245) | −66.30 (−65.58) |
| $[W_2Cl_9]^{3-}$ | RS | 3.440 (3.407) | −50.11 (−48.68) |
| | $S = 0$ | 2.426 (2.389) | −53.21 (−52.64) |
| | $S = 3$ | 3.440 (3.409) | −52.06 (−50.65) |
| | BS | 2.426 (2.390) | −53.21 (−52.63) |
| $[W_2Br_9]^{3-}$ | RS | 3.559 (3.540) | −46.21 (−44.73) |
| | $S = 0$ | 2.486 (2.413) | −49.05 (−48.45) |
| | $S = 3$ | 3.557 (2.541) | −48.07 (−46.62) |
| | BS | 2.486 (2.413) | −49.06 (−48.45) |
| $[W_2I_9]^{3-}$ | RS | 3.746 (3.726) | −41.77 (−40.54) |
| | $S = 0$ | 2.532 (2.468) | −44.25 (−43.77) |
| | $S = 3$ | 3.745 (3.727) | −43.53 (−42.29) |
| | BS | 2.533 (2.465) | −44.25 (−43.77) |

[a] The results of ZORA calculations are given in parentheses.

**4.1. Orbital Overlap and Spin Polarization in $[M_2X_9]^{3-}$ Species.** The results for orbital overlap ($\Delta E_{ovl}$) and spin polarization ($\Delta E_{spe}$) effects in the $[M_2X_9]^{3-}$ systems are summarized in Table 3. Also included are the values of the spin polarization energy ($^m\Delta E_{spe}$) for the corresponding monomeric $[MX_6]^{3-}$ complexes, which have been calculated as the difference in energy between the spin singlet and quartet states.

Qualitatively similar trends are observed for all four energy terms as the ligand is changed from fluoride, through chloride and bromide, to iodide. The values of the energy terms are found to decrease down the halide group, the most significant differences occurring between F and Cl (as also observed in the potential energy curves calculated for these systems[3]).

The changes in the spin polarization energy for both the monomers and dimers are equivalent to those observed in previous investigations of transition metal chloride systems.[2] For example, in the $[MCl_6]^{3-}$ series of group 6 (Cr, Mo, W) and group 7 (Mn, Tc, Re) elements, the complexes with larger metal ions or more covalent M−Cl interactions exhibit smaller values of the spin polarization energy, as these factors contribute to increasing the average interelectronic separation. Analogously, in the Mo and W $[MX_6]^{3-}$ series, the reduction

(10) ADF2002.01, SCM, Theoretical Chemistry, Vrije Universiteit, Amsterdam, The Netherlands (http://www.scm.com).
(11) Fonseca Guerra, C.; Snijders, J. G.; te Velde, G.; Baerends, E. J. *Theor. Chem. Acc.* **1998**, *99*, 391.
(12) te Velde, G.; Bickelhaupt, F. M.; van Gisbergen, S. J. A.; Fonseca Guerra, C.; Baerends, E. J.; Snijders, J. G.; Ziegler, T. *J. Comput. Chem.* **2001**, *22*, 931.
(13) Vosko, S. H.; Wilk, L.; Nusair, M. *Can. J. Phys.* **1980**, *58*, 1200.
(14) Kohn, W.; Sham, L. J. *Phys. Rev.* **1965**, *140*, A1133.
(15) Becke, A. D. *Phys. Rev. A* **1988**, *38*, 3098.
(16) Perdew, J. P. *Phys. Rev. B* **1986**, *33*, 8822.

**Table 3.** Overlap ($\Delta E_{ovl}$) Energy and Spin Polarization ($\Delta E_{spe}$) Energy Values (in eV) for $[M_2X_9]^{3-}$ Species[a]

| molecule | $\Delta E_{ovl}$ | $\Delta E_{spe}$ | $\Delta E_{spe} - \Delta E_{ovl}$ | molecule | $^{m}\Delta E_{spe}$ |
|---|---|---|---|---|---|
| $[Mo_2F_9]^{3-}$ | +3.60 | +2.43 | −1.17 | $[MoF_6]^{3-}$ | +1.32 |
| $[Mo_2Cl_9]^{3-}$ | +2.81 | +2.18 | −0.63 | $[MoCl_6]^{3-}$ | +1.13 |
| $[Mo_2Br_9]^{3-}$ | +2.53 | +2.10 | −0.43 | $[MoBr_6]^{3-}$ | +1.08 |
| $[Mo_2I_9]^{3-}$ | +2.18 | +1.98 | −0.20 | $[MoI_6]^{3-}$ | +1.03 |
| $[W_2F_9]^{3-}$ | +3.93 (+4.60) | +2.25 (+2.20) | −1.68 (−2.40) | $[WF_6]^{3-}$ | +1.19 (+1.21) |
| $[W_2Cl_9]^{3-}$ | +3.10 (+3.96) | +1.95 (+1.97) | −1.15 (−1.99) | $[WCl_6]^{3-}$ | +1.01 (+1.01) |
| $[W_2Br_9]^{3-}$ | +2.84 (+3.72) | +1.86 (+1.89) | −0.98 (−1.83) | $[WBr_6]^{3-}$ | +0.94 (+0.96) |
| $[W_2I_9]^{3-}$ | +2.48 (+3.23) | +1.76 (+1.75) | −0.72 (−1.48) | $[WI_6]^{3-}$ | +0.91 (+0.89) |

[a] The spin polarization energy ($^{m}\Delta E_{spe}$ in eV) of the corresponding $[MX_6]^{3-}$ complexes is also included for comparison. The results of ZORA calculations on W systems are given in parentheses.

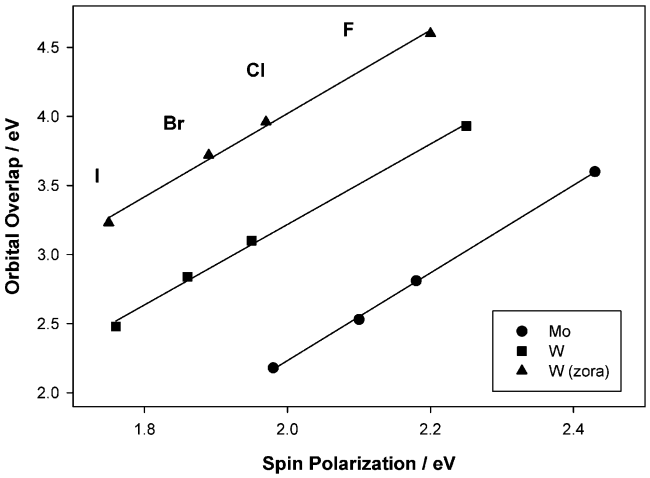


**Figure 4.** Variation of the overlap ($\Delta E_{ovl}$) energy as a function of the spin polarization ($\Delta E_{spe}$) energy in $[M_2X_9]^{3-}$ systems.

of the spin polarization energy upon descending the halide group can be associated with the increasing size and covalency of the ligand atoms which leads to more delocalized density and, thus, to greater average interelectronic separation.

A comparison of the spin polarization results for dimers and monomers reveals that the energy values are related by a factor of approximately 2 and, therefore, as found for the transition metal $[M_2Cl_9]^{z-}$ systems,[2] the spin polarization energy of the dimer appears to be largely determined by the sum of the contributions due to the individual metal centers.

The trends observed for the orbital overlap effects are different from those found for the transition metal chloride series previously investigated.[2] Plots of the overlap energy as a function of the spin polarization energy are shown in Figure 4. Although a strong linear correlation between the two factors is observed, the overlap energy values decrease as the spin polarization energy values do, whereas in the transition metal groups these terms vary in opposition to one another.

Upon descending a transition metal group, the greater size of the metal ions and the more diffuse nature of the metal orbitals lead to an enhancement of metal−metal overlap and to a reduction of the spin polarization energy. Therefore, the overlap and spin polarization terms are larger and smaller, respectively, for the heavier elements in the group. This is observed in the comparison of the results obtained for $[Mo_2X_9]^{3-}$ and $[W_2X_9]^{3-}$ systems for each individual halide element (Table 3 and Figure 4).

The trends observed for $[Mo_2X_9]^{3-}$ and $[W_2X_9]^{3-}$ systems down the halide group are similar to those found for $[M_2Cl_9]^{z-}$ dimers across a transition metal period.[2] A comparison of the results obtained for the transition metal triads previously studied reveals that the metal−metal separation is longer for group 7 elements than it is for group 6 elements, whereas both the overlap energy and spin polarization energy values are smaller. This is also the result obtained for the $[Mo_2X_9]^{3-}$ and $[W_2X_9]^{3-}$ systems upon descending the halide group. Increased metal−metal bond distances and decreased orbital overlap and spin polarization terms are observed in the heavier with respect to the lighter halide dimers.

A previous fragment analysis of the Mo and W $[M_2X_9]^{3-}$ systems has indicated that the metal−metal interaction energy is not strongly affected by changes in the ligands, even though the metal−metal bond length varies significantly within the halide group.[3] This result has been explained by considering that any decrease in the strength of the metal−metal interaction, upon descending the group, can be compensated by the increasing dilation of the metal d orbitals associated with metal−ligand covalency effects.

The fragment analysis of the Mo and W $[M_2X_9]^{3-}$ systems has been repeated using the optimized structures (for the $S = 0$ state) obtained in the present work. The results are shown in Table 4. The metal−metal, metal−bridge, and total interaction energy values have been obtained, respectively, by means of eqs 1−3. All fragment calculations have been

$$2[MX_3] = [M_2X_6] \quad (1)$$

$$[M_2X_6] + [X_3]^{3-} = [M_2X_9]^{3-} \quad (2)$$

$$2[MX_3] + [X_3]^{3-} = [M_2X_9]^{3-} \quad (3)$$

performed in a restricted manner, and the values of the metal−metal and total interaction energies have been subsequently corrected by incorporating the difference between the restricted and unrestricted results for the $[MX_3]$ species.

The results of the fragment analysis shown in Table 4 are different from those previously reported[3] in that the metal−metal interaction energy decreases slightly (instead of remaining largely constant[3]) as the halide group is descended and the metal−metal distance increases. However, the changes in the metal−bridge interaction energy are much greater and represent the dominant contribution to the variations in the total interaction energy (as previously observed[3]).

**Table 4.** Fragment Analysis (in kJ mol$^{-1}$) of Metal−Metal and Metal−Bridge Interactions, and Total Interaction Energy (in kJ mol$^{-1}$) for the $S = 0$ States of $[M_2X_9]^{3-}$ Species[a]

| | interaction energy | | |
|---|---|---|---|
| molecule | metal−metal $2[MX_3] = [M_2X_6]$ | metal−bridge $[M_2X_6] + [X_3]^{3-} = [M_2X_9]^{3-}$ | total $2[MX_3] + [X_3]^{3-} = [M_2X_9]^{3-}$ |
| $[Mo_2F_9]^{3-}$ | −202 | −1503 | −1705 |
| $[Mo_2Cl_9]^{3-}$ | −195 | −1095 | −1290 |
| $[Mo_2Br_9]^{3-}$ | −183 | −986 | −1169 |
| $[Mo_2I_9]^{3-}$ | −175 | −835 | −1010 |
| $[W_2F_9]^{3-}$ | −258 (−420) | −1475 (−1432) | −1733 (−1852) |
| $[W_2Cl_9]^{3-}$ | −253 (−383) | −1079 (−1110) | −1332 (−1493) |
| $[W_2Br_9]^{3-}$ | −242 (−365) | −964 (−1022) | −1206 (−1387) |
| $[W_2I_9]^{3-}$ | −233 (−337) | −841 (−922) | −1074 (−1259) |

[a] The results of ZORA calculations (at the nonrelativistic geometry) on W systems are given in parentheses.

Despite the comparatively small variation of the metal−metal interaction energy, the $S = 0$ and $S = 3$ states are increasingly destabilized by the change in the ligand from fluoride, through chloride and bromide, to iodide, as reflected by the decreasing values of the overlap and spin polarization terms.

It has been mentioned that the decreasing trend in spin polarization energy correlates with longer distances and more covalent character of the metal−ligand bonds which contribute to increasing the average separation between electrons. The decreasing trend in overlap energy appears to be an indirect effect in that, according to the results of the fragment analysis, it may be more closely related to the destabilization of the $S = 0$ state upon descending the halide group due to the destabilization of the metal−bridge interaction than it is to changes in the metal−metal interaction. (Across a transition metal period, the reduction in spin polarization energy can also be connected with changes in metal−ligand covalency, whereas the decrease in overlap energy may be explained by the contraction of the metal d orbitals reducing the metal−metal interaction.)

The energetic difference between the $S = 0$ and $S = 3$ states, which corresponds to the difference between the overlap and spin polarization terms (and is given as $\Delta E_{spe} - \Delta E_{ovl}$ in Table 3), can be used as an indication of the tendency of the metal-based electrons to delocalize or localize.

It has been mentioned that both states become destabilized upon descending the halide group, but this effect is actually more important for the overlap energy than the spin polarization energy, and is reflected by the diminishing (absolute) values of the $\Delta E_{spe} - \Delta E_{ovl}$ term.

The results in Table 3 show that the overlap energy is larger than the spin polarization energy for all Mo and W species, and are thus consistent with the nature of the respective potential energy curves,[3] which indicate that all systems exhibit some degree of metal−metal bonding or delocalization of the metal-based electrons. There are, however, significant differences between the $[Mo_2X_9]^{3-}$ and $[W_2X_9]^{3-}$ systems, and within the halide group.

For $[Mo_2X_9]^{3-}$ dimers, the minima in the broken-symmetry potential energy curves coincide with those in the $S = 0$ curves for F, Cl, and Br, suggesting a metal−metal triple bond. However, complete delocalization of the metal-based electrons can only be considered in the case of $[Mo_2F_9]^{3-}$, as the $S = 2$ curves for $[Mo_2Cl_9]^{3-}$ and $[Mo_2Br_9]^{3-}$ are also energetically close and thus suggest that decoupling of the $\delta_\pi$ electrons should be a relatively facile process. The values of the $\Delta E_{spe} - \Delta E_{ovl}$ term reflect this observation, being significantly less negative for the Cl and Br systems than for the F dimer. The results obtained for $[Mo_2I_9]^{3-}$ suggest that the most appropriate description of the Mo−Mo interaction is intermediate between a $\sigma$-bonded and a nonbonded structure (but closer to the former) and, therefore, that the metal-based electrons should be considerably more decoupled or localized than they are in the F, Cl, and Br systems. The $\Delta E_{spe} - \Delta E_{ovl}$ term for $[Mo_2I_9]^{3-}$ has the lowest value in the $[Mo_2X_9]^{3-}$ series, and corresponds to only a small energetic difference between the $S = 0$ and $S = 3$ states, which is consistent with this species exhibiting the greatest tendency toward localization of the metal-based electrons.

The minima in the potential energy curves for all $[W_2X_9]^{3-}$ dimers are coincident with the respective $S = 0$ curves, which lie significantly lower in energy than the $S = 2$ and $S = 3$ curves. These results are thus indicative of the presence of a strong metal−metal triple bond in all systems. In accord with this observation, the $\Delta E_{spe} - \Delta E_{ovl}$ term for the W dimers is dominated by the orbital overlap effects. The actual values are significantly more negative than those obtained for Mo dimers, but a similar decreasing trend, as the halide group is descended, is observed. This trend is consistent with the fact that, although the $S = 0$ state prevails over the $S = 2$ and $S = 3$ states in all four $[W_2X_9]^{3-}$ species, the latter become progressively more stabilized for the heavier systems and, consequently, the relative importance of the spin polarization and overlap terms increases and decreases, respectively.

**4.2. Relativistic Effects in $[W_2X_9]^{3-}$ Species.** Previous calculations have shown that inclusion of relativistic effects in the optimization of metal−metal bond distances normally leads to poorer agreement with experimental data.[1] A notable example is the $[Re_2Cl_9]^-$ system, with an observed[17−20] Re−Re separation of 2.70−2.73 Å. The results of nonrelativistic calculations employing local functionals have been found to be in excellent agreement with the experimental data, but the incorporation of relativistic corrections has led to a considerable underestimation of the metal−metal bond length, by as much as 0.3 Å.

The present results for the $[W_2X_9]^{3-}$ dimers show that use of the ZORA method[21−23] in geometry optimizations leads

(17) Heath, G. A.; McGrady, J. E.; Raptis, R. G.; Willis, A. C. *Inorg. Chem.* **1996**, *35*, 6838.
(18) Hauck, H. G.; Klingelhofer, P.; Muller, U.; Dehnicke, K. *Z. Anorg. Allg. Chem.* **1984**, *510*, 180.
(19) Baranov, A. I.; Khvorykh, G. V.; Troyanov, S. I. *Z. Anorg. Allg. Chem.* **1999**, *625*, 1240.
(20) Rabe, S.; Muller, U. *Z. Anorg. Allg. Chem.* **2000**, *626*, 830.
(21) van Lenthe, E.; Baerends, E. J.; Snijders, J. G. *J. Chem. Phys.* **1993**, *99*, 4597.
(22) van Lenthe, E.; Baerends, E. J.; Snijders, J. G. *J. Chem. Phys.* **1994**, *101*, 9783.
(23) van Lenthe, E.; Ehlers, A. E.; Baerends, E. J. *J. Chem. Phys.* **1999**, *110*, 8943.

to a shortening of the W−W distances for all states of all systems, with the sole exception of the reference and $S = 3$ states of $[W_2F_9]^{3-}$, but the differences between the nonrelativistic and ZORA values are relatively small. Nevertheless, for $[W_2Cl_9]^{3-}$, the former are in better agreement with available experimental data[24,25] indicating a W−W bond length of 2.41−2.44 Å.

The incorporation of ZORA relativistic corrections does not the change the orbital overlap and spin polarization trends on a qualitative level, as shown by the fact that largely similar linear correlations between the two terms are obtained with or without the ZORA effects (Figure 4). However, the overlap energy values become significantly larger with inclusion of relativistic corrections, whereas the spin polarization energy values are mostly unaffected. Therefore, use of the ZORA method results in an enhanced tendency toward strong coupling of the metal-based electrons as a consequence of the preferential stabilization of the $S = 0$ state with respect to the $S = 3$ state.

The inclusion of the ZORA relativistic corrections also has an important quantitative effect on the results of the fragment analysis, as the changes in the metal−metal interaction energy are significantly larger than those found in the nonrelativistic calculation, whereas the changes in the metal−bridge interaction energy are somewhat smaller than the corresponding nonrelativistic results. Nevertheless, despite these differences between ZORA and nonrelativistic treatments, the trends associated with the metal−bridge interaction remain the dominant component of the trends observed for the total interaction energy results.

**4.3. Orbital Overlap and Spin Polarization in $[M_2X'_3X''_6]^{3-}$ Species.** In our study of the orbital overlap and spin polarization effects in transition metal chloride systems,[2] we examined the properties of mixed-metal $[M'M''Cl_9]^{z-}$ species and found that their behavior fits almost exactly into the trends obtained for the regular $[M_2Cl_9]^{z-}$ species. In the present investigation, we have also considered mixed-ligand $[Mo_2X'_3X''_6]^{3-}$ systems, and in this section we compare their properties to those of the regular $[Mo_2X_9]^{3-}$ dimers analyzed in detail in the preceding sections.

Figure 5 contains a plot of the overlap energy as a function of the spin polarization energy for the F, Cl, and I $[Mo_2X_9]^{3-}$ dimers, and the corresponding F−Cl and Cl−I mixed-ligand systems. Although an approximate linear correlation is observed, this is of poorer quality than those obtained for the Mo and W $[W_2X_9]^{3-}$ species (Figure 4), and significant deviations (particularly for the F−Cl systems) are evident.

A possible explanation for these deviations in the behavior of the mixed-ligand dimers lies in the fact that, unlike the $[Mo_2X_9]^{3-}$ and $[W_2X_9]^{3-}$ species for which the variation of the structural and energetic properties exhibits high consistency throughout the entire ligand series, there are (important) irregularities in the changes in metal−metal distances and energy values of the $S = 0$ and $S = 3$ states of the $[Mo_2X'_3X''_6]^{3-}$ systems.

(24) Dunbar, K. R.; Pence, L. E.. *Acta Crystallogr.* **1991**, *C47*, 23.
(25) Watson, W. H.; Waser, J. *Acta Crystallogr.* **1958**, *11*, 689.

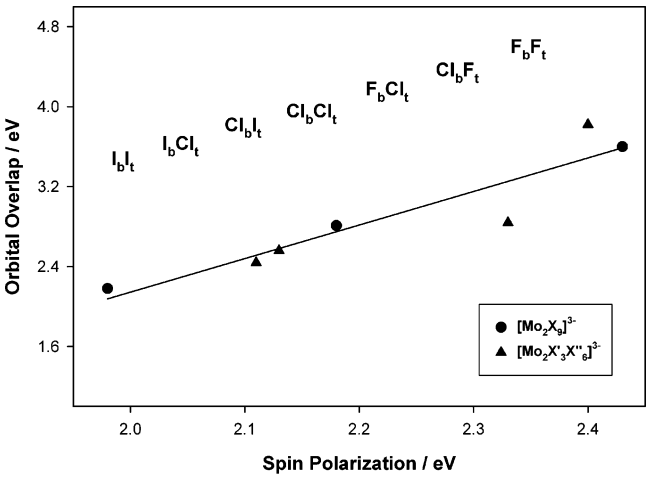


**Figure 5.** Variation of the overlap ($\Delta E_{ovl}$) energy as a function of the spin polarization ($\Delta E_{spe}$) energy in $[Mo_2X_9]^{3-}$ and $[Mo_2X'_3X''_6]^{3-}$ systems. The b and t subscripts label ligands occupying bridging and terminal positions, respectively.

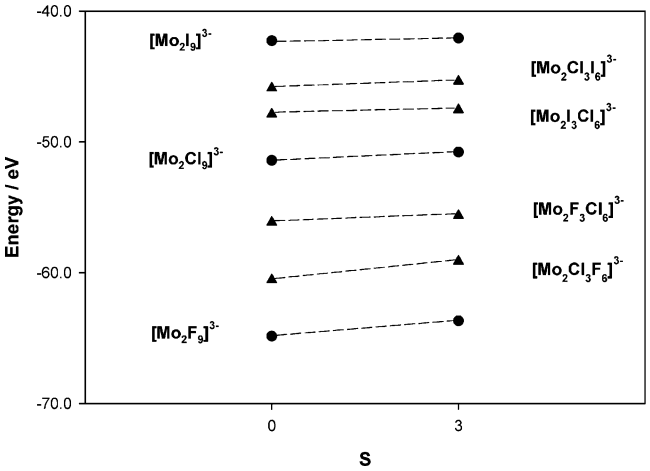


**Figure 6.** Total bonding energy ($E_B$) values for the $S = 0$ and $S = 3$ states of $[Mo_2X_9]^{3-}$ and $[Mo_2X'_3X''_6]^{3-}$ systems.

An example of the structural changes observed in the mixed-ligand systems can be found in a comparison of $[Mo_2F_3Cl_6]^{3-}$ with $[Mo_2F_9]^{3-}$ and $[Mo_2Cl_3F_6]^{3-}$ with $[Mo_2Cl_9]^{3-}$. The Mo−Mo distances in the $S = 0$ and $S = 3$ states are longer and shorter, respectively, in $[Mo_2F_3Cl_6]^{3-}$ than $[Mo_2F_9]^{3-}$, whereas the opposite result is found for $[Mo_2Cl_3F_6]^{3-}$, as this species has a shorter Mo−Mo bond in the $S = 0$ state but a longer Mo−Mo bond in the $S = 3$ state than $[Mo_2Cl_9]^{3-}$.

The energy of the $S = 0$ and $S = 3$ states is plotted in Figure 6 for the F, Cl, and I $[Mo_2X_9]^{3-}$ and the F−Cl and Cl−I $[Mo_2X'_3X''_6]^{3-}$ systems. Although the values obtained for the mixed-ligand species lie in intermediate positions, between those for the corresponding $[Mo_2X_9]^{3-}$ dimers, it is their relative stability (with respect to the reference states) that affects the overlap and spin polarization terms, and leads to the observed deviations. For $[Mo_2Cl_3I_6]^{3-}$ and $[Mo_2I_3Cl_6]^{3-}$, these deviations are small and the results are relatively close to those which would be predicted by extrapolation from $[Mo_2Cl_9]^{3-}$ and $[Mo_2I_9]^{3-}$. However, the behavior of the $[Mo_2F_3Cl_6]^{3-}$ and $[Mo_2Cl_3F_6]^{3-}$ systems deviates consider-

ably from the results obtained for the regular $[Mo_2F_9]^{3-}$ and $[Mo_2Cl_9]^{3-}$ dimers.

If $[Mo_2F_9]^{3-}$ is used as a reference, the comparatively small value of the overlap energy in $[Mo_2F_3Cl_6]^{3-}$ (which is similar to that of $[Mo_2Cl_9]^{3-}$ even though the spin polarization energy values are significantly different) can be related to the fact that the structural and bonding changes lead to a relative stabilization of the $S = 3$ state with respect to the $S = 0$ state, the $\Delta E_{spe} - \Delta E_{ovl}$ terms being $-0.51$ and $-1.17$ eV for $[Mo_2F_3Cl_6]^{3-}$ and $[Mo_2F_9]^{3-}$, respectively.

The opposite result is found for $[Mo_2Cl_3F_6]^{3-}$. A relative stabilization of the $S = 0$ state with respect to the $S = 3$ state causes the overlap energy to become considerably greater than it is for $[Mo_2F_9]^{3-}$ (as reflected by the respective $\Delta E_{spe} - \Delta E_{ovl}$ terms which have values of $-1.42$ and $-1.17$ eV), despite the results for the spin polarization energy for these species being only slightly different.

## 5. Conclusion

The influence of the ligand on the coupling between the metal-based electrons in $d^3d^3$ face-shared $[Mo_2X_9]^{3-}$ and $[W_2X_9]^{3-}$ systems has been investigated by calculating orbital overlap and spin polarization effects for the F, Cl, Br, and I species. As previously found for the transition metal triads, a strong linear correlation between these factors has been observed, and the general trends obtained are consistent with the nature of the potential energy curves for these systems.

The values of the overlap and of the spin polarization terms have been found to diminish as the halide group is descended. The decreasing trend in the spin polarization energy can be related to the increasing size and covalency of the ligand, whereas the decreasing trend in the overlap energy appears to be mostly associated with the effects of the metal−bridge interaction on the stability of the $S = 0$ state. The inclusion of relativistic effects in the treatment of $[W_2X_9]^{3-}$ systems has been found to change the values of the structural and energetic parameters, but not to affect the general qualitative trends.

In addition to the regular $[M_2X_9]^{3-}$ systems, certain mixed-ligand species have also been studied. A correlation between the orbital overlap and spin polarization terms has also been observed in the mixed-ligand species, but it is not as strong as in the regular systems, and significant deviations have been found, in particular $[Mo_2F_3Cl_6]^{3-}$ and $[Mo_2Cl_3F_6]^{3-}$. These deviations can be related to structural and energetic characteristics that do not fit entirely into the trends obtained for the $[M_2X_9]^{3-}$ series.

**Acknowledgment.** Financial support from the Australian Research Council is gratefully acknowledged.

IC026291P